

Electrochemical Behaviour of Apoferritin Encapsulating of Silver(I) Ions and Its Application for Treatment of *Staphylococcus aureus*

Dana Dospivova¹, David Hynek^{1,2}, Pavel Kopel^{1,2}, Andrea Bezdekova¹, Jiri Sochor^{1,2}, Sona Krizkova^{1,2}, Vojtech Adam^{1,2}, Libuse Trnkova^{1,2,3}, Jaromir Hubalek^{1,2,4}, Petr Babula^{1,2}, Ivo Provaznik^{5,6}, Radimir Vrba^{2,4}, Rene Kizek^{1,2,3*}

¹ Department of Chemistry and Biochemistry, Faculty of Agronomy, Mendel University in Brno, Zemedelska 1, CZ-613 00 Brno, Czech Republic, European Union

² Central European Institute of Technology, Brno University of Technology, Technicka 3058/10, CZ-616 00 Brno, Czech Republic, European Union

³ Department of Chemistry, Faculty of Science, Masaryk University, Kotlarska 2, CZ-611 37 Brno, Czech Republic, European Union

⁴ Department of Microelectronics

⁵ Department of Biomedical Engineering, Faculty of Electrical Engineering and Communication, Brno University of Technology, Technicka 3058/10, CZ-616 00 Brno, Czech Republic, European Union and

⁶ International Clinical Research Center - Center of Biomedical Engineering, St. Anne's University Hospital Brno, Pekarska 53, CZ-656 91 Brno, Czech Republic, European Union

*E-mail: kizek@sci.muni.cz

Received: 8 May 2012 / Accepted: 12 June 2012 / Published: 1 July 2012

Methicillin-resistant *Staphylococcus aureus* (MRSA) is responsible for several difficult-to-treat infections in humans. Therefore, it is not surprising that other ways how to treat these bacteria are looked for. Silver(I) ions and silver nanoparticles exhibited the highest antimicrobial activity against MRSA but their transporting to the place of needs and *in situ* determination is an issue. The aim of this work was electrochemical determination of silver(I) ions using four types of modified carbon paste electrodes (CPEs) with different content of carbon nanoparticles. CPE made from expanded carbon was the most sensitive one. Therefore, we optimized the experimental conditions as time of accumulation 60 s, deposition potential 0.5 V and 0.2 M acetate buffer, pH = 5.0 to obtain detection limit (3 S/N) of 5 nM for silver(I) ions. Further, we studied the encapsulation of silver(I) ions into apoferritin as a possible way for transportation of these ions. Primarily we optimized the encapsulation conditions to prepare the most stable complex, which was subsequently utilized for treatment of *S. aureus*. Based on the results obtained it can be concluded that silver(I) ions remain enclosed in the apoferritin structure until decomposition of apoferritin by bacterial enzymatic apparatus occurs.

Keywords: electrochemical detection; silver; nanomaterial; nanomedicine

1. INTRODUCTION

Silver in ionic form, together with colloidal silver particles, belongs to the most important environmental contaminants. Silver ions are released into the quarry waters as a consequence of silver and other metal ores processing and also in sewage water from photographic and jewellery industry (cyanide silvering). Waste from glass industry, electrochemical industry and health service are other important sources of silver ions releasing to environment [1]. All soluble and colloidal silver forms are highly toxic, especially for aquatic environment and the whole water ecosystem [2,3]. Determination of Ag^+ ions is therefore much needed. There are many methods utilizable for Ag^+ quantification from colorimetric and optical ones [4,5], atomic absorption spectroscopy (AAS) as the most widely used [6-8], to electrochemical methods and biosensors [9,10] and inductively coupled plasma mass spectrometry (ICP-MS) [11,12]. Single-pulse Laser-Induced Breakdown Spectroscopy (LIBS) and Laser-Ablation Inductively Coupled Plasma Mass-Spectrometry (LA-ICP-MS) belongs to methods usable for silver imaging in animal or plant tissues [13].

In spite of the fact that AAS is the most widely used method for determination of silver(I) ions, electrochemical methods offer a rapid and low-cost possibility of relatively simple Ag^+ determination with sensitivity comparable to AAS [14]. Carbon tip, carbon-paste and glassy carbon electrodes are applicable for Ag^+ determination in biological matrix, like plant or fish tissues and environmental samples [15-28]. Carbon nanotube electrodes offer possibilities for further improvement of detection limit of Ag^+ . There are also some indirect possibilities how to determine silver(I) ions including determination of heavy metal binding protein metallothionein (MT) [29]. High affinity of MT for Ag^+ was also utilized for construction of a simple biosensor for Ag^+ ions detection [28,30-32].

Besides the role of Ag^+ ions in the contamination of the environment, these ions have found important position in biotechnological and medical applications. The antimicrobial activity of silver nanoparticles has been investigated. Their bactericide effect was shown in numerous papers. These nanomaterials, which can be prepared in a simple and cost-effective manner, may be suitable for the formation of new types of bactericidal materials, like silver-coated textiles and doped phenyltriethoxysilane sol-gel coating [33-37]. Silver preparations and nanoparticles offer an alternative to antibiotics due to increasing bacterial antibiotics resistance. Methicillin-resistant *Staphylococcus aureus* (MRSA) is responsible for several difficult-to-treat infections in humans. This bacterium causes severe infection in immune compromised patients, especially in hospitals, nursing homes and other medical facilities. Silver(I) ions and silver nanoparticles exhibited the highest antimicrobial activity against MRSA followed by methicillin-resistant *Staphylococcus epidermidis* and *Streptococcus pyogenes*, whereas only moderate antimicrobial activity was found against *Salmonella typhi* and *Klebsiella pneumoniae* [38-40]. For these purposes, the most suitable modern ways of preparation of silver(I) ions are intensely searched. Other application of silver nanoparticles with photocatalytic activity are removal of pesticides and other toxic matters from environment [41] or production of hydrogen from water [42]. Therefore, options for transporting silver(I) ions to the place of needs are sought. Liposomes belong to very often studied transportation systems, especially, due to their

applications for drug delivery and better effectiveness of therapy. Apoferritins are another group of tested compounds. Apoferritin is a protein composed of 24 polypeptide subunits that form a cage like structure with 12.5 nm diameter and cavity of approximately 8 nm. In the interior there can be placed up to 4500 iron atoms in the form of iron oxide-hydroxide. There are 14 channels in the structure of apoferritin that can be used for diffusion of ions into the cage [43]. This unique structure has been used for synthesis of wide spectrum of nanoparticles or nanoalloys. Drug delivery of cisplatin, carboplatin, oxaliplatin or daunomycin by apoferritin was studied by Xing [44] and Ma-Ham [45]. Nanoparticles of CeO₂ [46], MnOOH [47], Gd [48,49] and Eu [50] complexes in apoferritin cage were tested as magnetic resonance imaging contrast agents. Phosphate nanoparticles prepared in apoferritin cavity as tags for bioanalytical or product tracking identification were reported by Liu et al. [51-54].

The aim of this work was electrochemical determination of silver(I) ions using various types of modified carbon paste electrodes with different content of carbon nanoparticles. The most suitable procedure was used for determination of free silver(I) ions capped in the apoferritin structure.

2. EXPERIMENTAL PART

2.1 Chemicals and material

Four types of carbon powder were used in this study. Two types of spherical glassy carbon powder were 2-12 μm and 10-40 μm of diameter. One type was multiwalled carbon nanotube (MWCNT) with parameters: O.D. \times length 6-13 nm \times 2.5-20 μm . These three powders were purchased from Sigma-Aldrich (USA). Fourth carbon material was expanded carbon obtained from Brno University of Technology, Brno, Czech Republic. All other used reagents were purchased from Sigma-Aldrich (USA) in ACS purity. To pipette volumes down to micro and nanolitres, pipettes used were purchased from Eppendorf Research (Eppendorf, Germany) with the highest certified deviation ($\pm 12\%$). The deionised water was prepared using reverse osmosis equipment Aqual 25 (Aqual, Czech Republic). The deionised water was further purified by using apparatus MiliQ Direct QUV equipped with the UV lamp. The resistance was 18 M Ω . The pH was measured using pH meter WTW inoLab (Weilheim, Germany).

2.2 Electrochemical analysis

Electrochemical measurements were performed using a CH Instruments Electrochemical Workstation (CH Instruments, USA), using glass cell with three electrodes. Various types of carbon paste electrodes were tested as working electrodes. The reference electrode was Ag/AgCl/3M KCl (Metrohm, Switzerland) and the counter electrode was made of platinum (Metrohm, Switzerland). The differential pulse voltammetry (DPV) parameters were as follows: initial potential -0.2 V, end potential 0.5 V, modulation amplitude 0.05 V, step potential 0.001 V. All experiments were carried out at room

temperature. Acetate buffer (0.2 M, pH 5.0) was used as the supporting electrolyte. Every measuring solution consisted from 10 μ l of sample and 1990 μ l of acetate buffer. For results evaluation software CHI 440A was used.

2.3 Preparation of carbon paste electrodes

The unmodified carbon paste electrode was prepared by mixing graphite powder with appropriate amount of mineral oil (Sigma Aldrich) and through hand mixing in a mortar and pestle (~75:25 %, w/w). A portion of the composite mixture was packed into the end of a teflon tube. The carbon nanotube-carbon paste composite electrode was also prepared according to the same procedure, using an appropriate amount of MWCNT, which was transferred and mixed thoroughly with unmodified carbon paste. For carbon of the size 2-12 μ m (electrode name CNT2_12) and 6-13 μ m (electrode name CNT6_13), the rate was as follows: 1.0 g of carbon and 300 μ l of oil (70/30 %, w/v), in the case of paste (carbon 10-40 μ m, electrode name CNT10_40) the carbon:oil rate was 50/50 % (1.0 g of carbon and 500 μ l of mineral oil, w/v). For the expanded carbon, the amount of 0.1 g was mixed with a volume of 300 μ l of mineral oil (electrode name CPE_Expa). Carbon powder was homogenized in an agate mortar for 25 min. The carbon paste was housed in a teflon body having a 2.5 mm diameter of active disk surface.

2.4 Preparation of apoferritin nanoparticles

Apoferritin solution (0.25 mg/ml, equine spleen, Sigma-Aldrich) was filtered through Microcon YM-30 to remove aggregates. Filtrate was diluted with ACS water and centrifuged on a centrifugal filter device Amicon Ultra 3k (Millipore) at 10,000 rpm and 10 °C using Centrifuge 5417R (Eppendorf, Germany). Apoferritin was washed several times with ACS water on the same filter. Other experimental conditions are in Results and discussion section.

2.5 Cultivation of bacterial strains and growth curves

Staphylococcus aureus (NCTC 8511) was obtained from the Czech Collection of Microorganisms, Faculty of Science, Masaryk University, Brno, Czech Republic. Strains were stored as a spore suspension in 20% (v/v) glycerol at -20 °C. Prior to use in this study, the strains were thawed and the glycerol was removed by washing with distilled water. The bacterial strain was incubated in the presence of cultivation medium (meat peptone 5 g/l, NaCl 5 g/l, bovine extract 1.5 g/l, yeast extract 1.5 g/l (HIMEDIA, Mumbai, India)), sterilized MiliQ water with 18 M Ω) at 600 rpm and 37 °C in Incubator Hood TH 15 (Edmund Buhler GmbH, Hechingen, Germany). pH of the cultivation medium was adjusted at 7.4 before sterilization. Sterilization was carried out at 121 °C for 30 min. in

sterilizer (BMT, Brno, Czech Republic). Grown bacterial culture was diluted by cultivation medium to $OD_{600} = 0.1$ prior to use in the following experiments. The prepared medium (10 ml) was pipetted into 25 ml flasks and apoferritin solution with Ag(I) ions (7.5, 15, 30 and 60 μM) was added.

Solutions containing bacteria and cultivation medium were mixed and pipetted (250 μl) into plastic plate (MaxiSorp, NUNC Immuno, Denmark). Subsequently, apoferritin containing silver(I) ions at the concentrations of 0, 7.5, 15, 30 and 60 μM was added (applied volume of 50 μl). A spectrometer device Multiscan EX (Thermo Fischer, Germany) was used for measuring of the solution absorbance at 620 nm every 30 min, 2 min. shake 800 rpm, total cultivation time 24 hours. All measurements were done in five replicates. Cuvette area was thermostated throughout the experiment to 37 °C (home-made temperature control box). The device was controlled by the Ascent Software version 2.6 program package (Thermo Fischer, Germany).

2.6 Mathematical treatment of data and estimation of detection limits

Data were processed using MICROSOFT EXCEL® (USA) and STATISTICA.CZ Version 8.0 (Czech Republic). Results are expressed as mean \pm standard deviation (S.D.) unless noted otherwise (EXCEL®). Statistical significances of the differences in growth of bacteria were determined using STATISTICA.CZ. Differences with $p < 0.05$ were considered significant and were determined by using of multifactorial ANOVA test (particularly Scheffe test), which was applied for means comparison. The detection limits (3 signal/noise, S/N) were calculated [55], whereas N was expressed as standard deviation of noise determined in the signal domain unless stated otherwise.

3. RESULTS AND DISCUSSION

Solid electrodes are routinely used in the field of electroanalytical chemistry. A carbon paste electrode (CPE) represents one of the mostly used electrodes [23,56-66]. One of the most important advantages of CPE is the possibility of its modification by both low-molecular and high-molecular mass compounds including enzymes and nucleic acids [23,67-70].

3.1 Carbon particles in carbon paste electrode

Carbon nanotubes (CNTs) have been under scientific investigation for more than fifteen years because of their unique properties that predestine them for many potential applications. The reason consists not only in mediation of reaction course, which has disadvantageous conditions on the surface of unmodified electrode, but also concentration of reactant on the electrode surface and especially biochemical reactions directly on the electrode (CPE) surface [68-71]. Presently, the limits of determination for unmodified CPE varies from $1 \cdot 10^{-6}$ to $1 \cdot 10^{-7}$ M [15,72]. The field of nanotechnology

and nanoscience push their investigation forward to produce CNTs with suitable parameters for future applications. It is evident that new approaches of their synthesis need to be developed and optimized [73]. MWCNTs were successfully prepared by using plasma enhanced chemical vapour deposition. Further, three carbon composite electrodes with different content of carbon particles with various shapes and sizes were prepared and tested on measuring of nucleic acids. Carbon composite electrode prepared from a mixture of glassy and spherical carbon powder and MWCNTs had the highest sensitivity to nucleic acids [74]. The great attention is paid to the questions of carbon particles and their application for determination of many analytes [75-78]. Carbon paste electrodes were prepared in accordance with procedure described in Material and Methods section Preparation of CPE modified by nanoparticles was simplified and consisted of mixture of carbon powders without organic solvent (dichloromethane) addition [78].

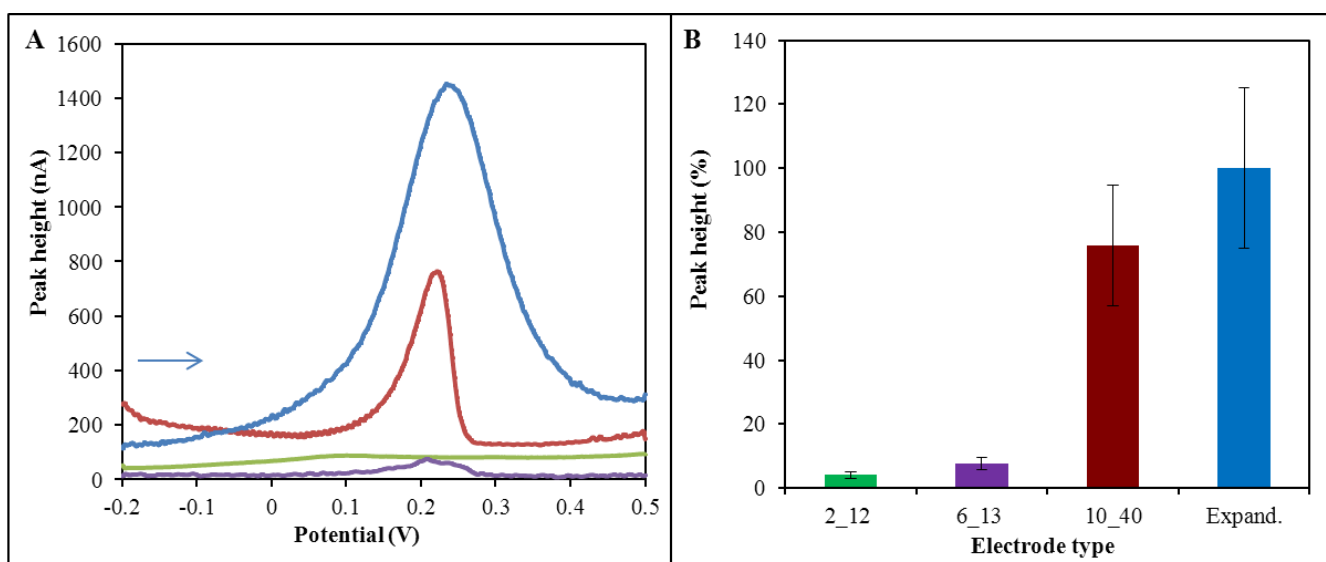


Figure 1. (A) Typical differential pulse voltammograms of silver(I) ions measured by various types of carbon paste electrodes as CNT2_12, CNT6_13, CNT10_40 and CPE_Expa). (B) Height of silver(I) ions peaks measured by various types of CPE re-calculated on the peak height measured by CPE_Expa, which was considered as 100 %. Concentration of silver ions was 5 μM . DPV parameters were as follows: initial potential -0.2 V, end potential 0.5 V, amplitude 0.05 V, pulse width 0.005 s, pulse period 0.05 s. Acetate buffer (0.2 M, pH 5.0) was used as a supporting electrolyte.

The aim of this part of the study was to determine possible electrochemical effect of like this prepared CPE (without complicated procedure of preparation). Prepared electrodes (CNT2_12, CNT6_13, CNT10_40 and CPE_Expa) were subsequently used for silver ions analysis (5 μM). The optimized procedures and techniques were followed from our previously published papers [15,30]. There are typical voltammograms of silver(I) ions in Fig. 1A. Characteristic potential of silver(I) ions

measured at tested electrodes were as follows: CNT2_12: 0.09 ± 0.02 V, CNT6_13: 0.22 ± 0.04 V, CNT10_40: 0.21 ± 0.03 V and CPE_Expa: 0.24 ± 0.04 V ($n = 5$). All four types of carbon paste were compared with respect to obtained signal of silver(I) ions. The highest signal was detected for expand carbon. For comparison with the rest of matrices, this value was considered as 100 %. The second highest response was determined for glassy carbon 10-40 μm paste - about 75 % of expand carbon signal. Remaining two matrices showed signals of 8 % (MWNT) and 4 % (CNT2_12) compared to expand carbon (Fig. 1B). It clearly follows from the results obtained that the most intensive responses of silver(I) ions were observed on CPE_Expa. This fact may be explained by dramatic enhancement of active surface of the electrode. Relative error between individual intraday analyses varied from 10 to 20 % ($n=5$), interday relative error was 15-25 % ($n=5$).

3.2 Optimization of silver(I) ions detection

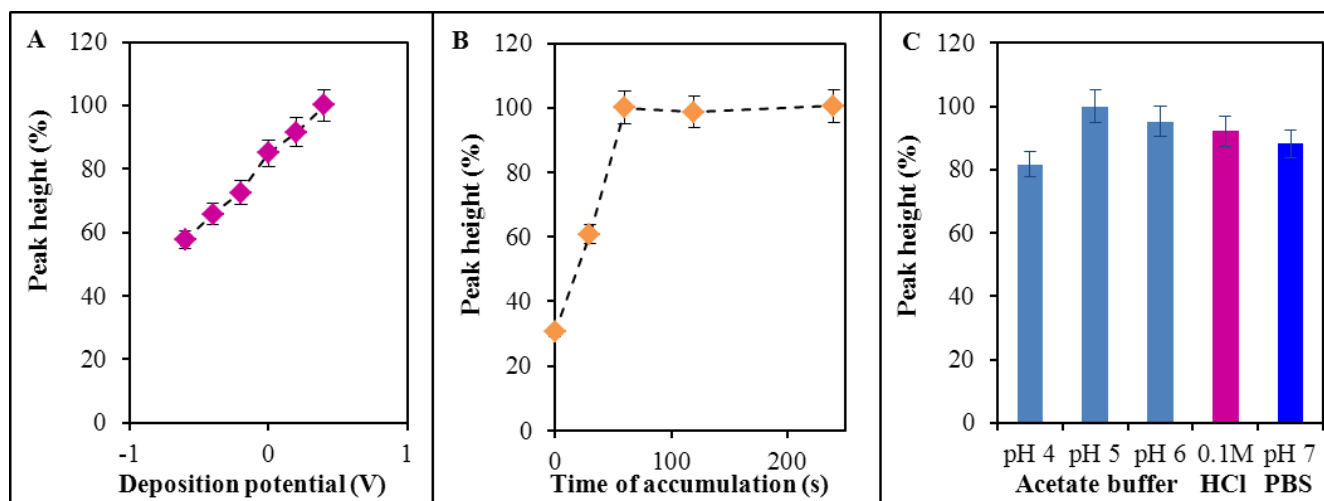


Figure 2. Optimization of silver electrochemical detection by tested CPEs (CNT2_12, CNT6_13, CNT10_40 and CPE_Expa). Data are represented as average values of obtained dependences from three independent analyses. (A) The effect of deposition potential on silver(I) ions peak. Time of accumulation: 120 s, 0.2 M acetate buffer pH 5. (B) The effect of time of accumulation on silver(I) ions peak. Deposition potential: 0.5 V, 0.2 M acetate buffer pH 5.0. (C) The effect of supporting electrolyte on silver(I) ions peak. Deposition potential: 0.5 V, time of accumulation 60 s.

The effect of deposition potential on the maximal electrode response of silver(I) ions ($5 \mu\text{M}$) for values of -0.6; -0.4; -0.2; 0; 0.2 and 0.5 V at the accumulation time 120 s was investigated. The observed signals for tested CPE modifications (CNT2_12, CNT6_13, CNT10_40 and CPE_Expa) increased with maximal value at the potential of 0.5 V (Fig. 2A). The results are presented as average for all types of electrodes. Further, the effect of time of accumulation (0, 30, 60, 120 and 240 s) under the accumulation potential of 0.5 V was studied.

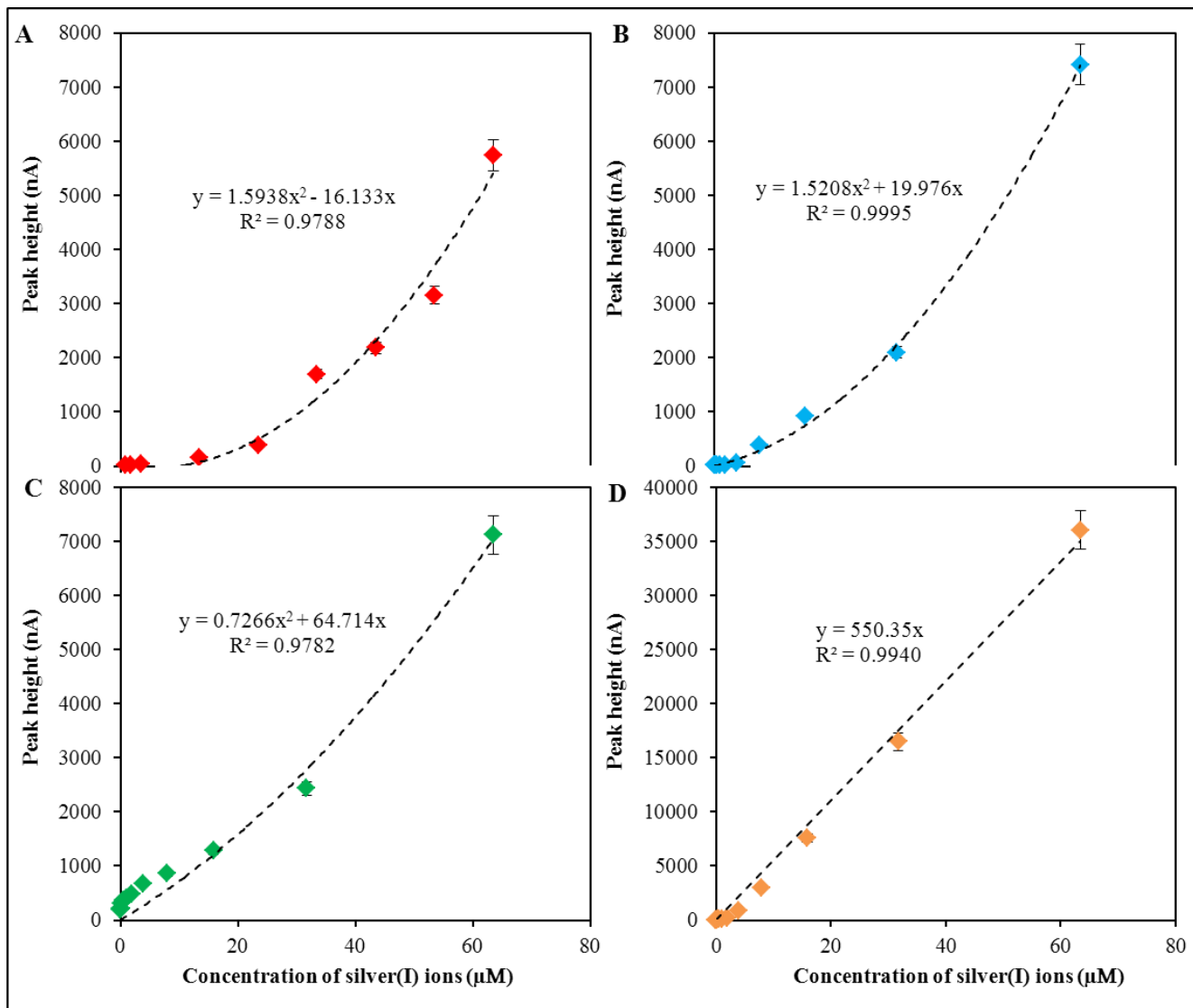


Figure 3. Calibration curves for silver(I) ions measured by CPEs made from (A) CNT2_12 – spherical glassy carbon 2-12 µm; (B) CNT6_13 – multiwalled nanotube 6-13 nm; (C) CNT10_40 – spherical glassy carbon 10-40 µm; (D) CPE_Expa – expanded carbon. DPV parameters were as follows: initial potential -0.2 V, end potential 0.5 V, amplitude 0.05 V, pulse width 0.005 s, pulse period 0.05, time of accumulation 60 s, deposition potential 0.5 V and 0.2 M acetate buffer, pH = 5.0.

Rapid increase of silver(I) ions signal was observed up to 60 s of the accumulation. Longer times of accumulation caused negligible changes in silver(I) ions signals, and, in addition, relative standard deviation (R.S.D.) increased from 5 % to 8 % (Fig. 2B). The effect of supporting electrolyte was studied too. In comparison of three different supporting electrolytes as acetate buffer (pH = 4.0; 5.0; 6.0), phosphate buffered saline (PBS, pH = 7.0) and 0.1 M HCl (pH 6.5), the acetate buffer proved the best characteristics for silver(I) ions detection (Fig. 2C). Slightly acidic pH of acetate buffer as a supporting electrolyte probably improves protonization of silver(I) ions and their subsequent

interaction with CPE. Using acetate buffer, the results were very well repeatable (compared to pH = 4.0). In the case of PBS and HCl buffers, shift of characteristic signal of silver(I) ions from 0.2 V to 0.03 – 0.04 V occurred. As optimal for subsequent determination of silver(I) ions using DPV on CPE the following parameters were chosen: time of accumulation 60 s, deposition potential 0.5 V and 0.2 M acetate buffer, pH = 5.0.

Tested CPEs were used for measurement of calibration dependences of silver(I) ions peaks heights on their concentrations within the range from 0.05 to 65 μM . The calibration curves measured at CNT2_12, CNT6_13, CNT10_40 and CPE_Expa are shown in Figs. 3A, B, C and D. Calibration dependences were interlayed with the most suitable curves with respect of maximal value of coefficient of determination.

In the case of carbon matrices (GC and MWNT), calibration dependences are interlayed by polynomial dependence of degree 2. The highest value of coefficient of determination was specified for MWNT with the value of $R^2 = 0.999$. Values of coefficient of determination for GC were lower as 0.978 for both types of GC.

Table 1. Analytical parameters of electrochemical determination of silver(I) ions with CPE called CNT2_12.

Substance	Regression equation	Dynamic range (μM)	Dynamic range ($\mu\text{g/ml}$)	R^2 ¹	LOD ² (μM)	LOD ($\mu\text{g/ml}$)	LOQ ³ (μM)	LOQ ($\mu\text{g/ml}$)	RSD ⁴ (%)
Ag	$y = 1.5938x^2 - 16.133x$	0.11 – 63.5	0.012 – 6.85	0.979	10	1	40	4	6.8

- 1...regression coefficients
- 2...limit of detection (3 S/N)
- 3...limits of quantification (10 S/N)
- 4...relative standard deviation

Table 2. Analytical parameters of electrochemical determination of silver(I) ions with CPE called CNT6_13.

Substance	Regression equation	Dynamic range (μM)	Dynamic range ($\mu\text{g/ml}$)	R^2 ¹	LOD ² (μM)	LOD ($\mu\text{g/ml}$)	LOQ ³ (μM)	LOQ ($\mu\text{g/ml}$)	RSD ⁴ (%)
Ag	$y = 1.5208x^2 + 19.976x$	0.03 – 63.5	0.003 – 6.85	0.998	0.3	0.03	1	0.1	9.0

- 1...regression coefficients
- 2...limit of detection (3 S/N)
- 3...limits of quantification (10 S/N)
- 4...relative standard deviation

Table 3. Analytical parameters of electrochemical determination of silver(I) ions with CPE called CNT10_40.

Substance	Regression equation	Dynamic range (μM)	Dynamic range ($\mu\text{g/ml}$)	R^2 ¹	LOD ² (μM)	LOD ($\mu\text{g/ml}$)	LOQ ³ (μM)	LOQ ($\mu\text{g/ml}$)	RSD ⁴ (%)
Ag	$y = 0.7266x^2 + 64.714x$	0.03 – 63.5	0.003 – 6.85	0.978	0.1	0.01	0.4	0.04	10.8

- 1...regression coefficients
- 2...limit of detection (3 S/N)
- 3...limits of quantification (10 S/N)
- 4...relative standard deviation

Table 4. Analytical parameters of electrochemical determination of silver(I) ions with CPE called CPE_Expa.

Substance	Regression equation	Dynamic range (μM)	Dynamic range ($\mu\text{g/ml}$)	R^2 ¹	LOD ² (μM)	LOD ($\mu\text{g/ml}$)	LOQ ³ (μM)	LOQ ($\mu\text{g/ml}$)	RSD ⁴ (%)
Ag	$y = 550.35x$	0.004 – 63.5	0.0004 - 6.85	0.991	0.005	0.0005	0.02	0.002	4.9

1...regression coefficients

2...limit of detection (3 S/N)

3...limits of quantification (10 S/N)

4...relative standard deviation

Expanded carbon as the only material provides calibration dependence of linear character with regression equation $y = 550.35x$, $R^2 = 0.994$. In the case of expanded carbon, limit of detection was 5 nM. Complete analytical parameters for CNT2_12, CNT6_13, CNT10_40 and CPE_Expa are summarized in Tabs. 1, 2, 3 and 4, respectively.

3.3 Encapsulating of silver(I) ions into apoferritin structure

Encapsulating of silver(I) ions into apoferritin structure constituted further step in our study (Fig. 4). Four concentrations of silver(I) ions were used for investigation of preparation procedure. Purified apoferritin was recovered and ACS water was added to the final volume of 3 ml. AgNO_3 (500 μl of 10 mM) was slowly added to apoferritin. The mixture was shaken (Vortex Genie2 (Scientific Industries, USA) for 1 h letting the silver(I) ions to diffuse into the cavity of the apoferritin (Fig. 4A). Subsequently, the solution was divided in two parts. To the first part 250 μl of 0.2 M phosphate buffer (pH = 7.0) was slowly added to form a silver phosphate inside the apoferritin (Fig. 4B), while the second part (Fig. 4A) was diluted with 250 μl of water only. The samples were shaken for 30 min and then centrifuged at 10,000 rpm. The supernatant was used for voltammetric measurements. Samples (Fig. 4A) and (Fig. 4B) were prepared with apoferritin without purification. Variant "A" represents mixture of apoferritin with silver(I) ions, when opening of apoferritin structure with subsequent releasing of silver(I) ions occurred after addition of acetate buffer (pH = 5.0). The released silver(I) ions can be detected electrochemically. Variant "B" represents the same mixture, but with addition of phosphate, when higher pH (pH = 7.0) causes enclosure of apoferritin structure. This fact may clarify only minimal detected signal of silver(I) ions. Further, we tested the influence of purification of apoferritin on the encapsulating of silver(I) ions according to both schemes, i.e. water only (Fig. 4C) and phosphate buffer (Fig. 4D). The results obtained were in good agreement with those obtained without purification.

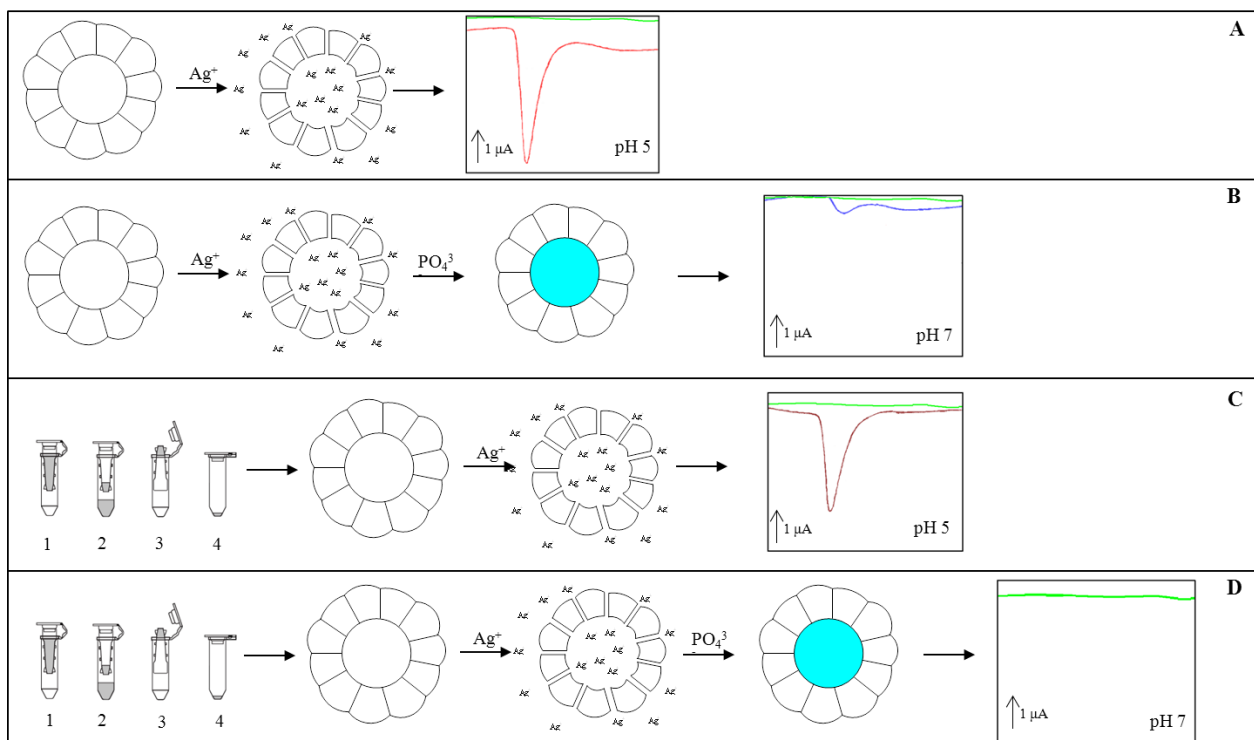


Figure 4. Scheme of the preparation of silver phosphate nanoparticles. (A) Apoferritin with AgNO_3 (10 mM), silver(I) ions diffused into the apoferritin cavity, electrochemical measurement of silver(I) ions; (B) apoferritin with AgNO_3 (10 mM) and phosphate buffer, formation of silver phosphate, electrochemical measurement of remaining silver(I) ions; (C) and (D) the same procedure as in the part (A) and (B), respectively, but with the purification of apoferritin before addition of silver(I) ions. Purification of apoferritin: 1) apoferritin diluted with ACS water filled in the filter device, 2) centrifugation at 10 000 rpm (10 °C), 3) recovery of purified apoferritin, 4) collecting sample of apoferritin.

In the unpurified apoferritin/silver ions mixture, the detected signals of silver(I) ions were for about 20-30 % lower compared to corresponding applied concentrations. Silver(I) ions surplus had to be removed to take advantage of apoferritin carrier as a mark based on heavy metal. Changes in silver(I) ions signals were caused by the binding-enclosure of silver(I) ions in apoferritin structure. Purification was based on the membrane permeability of metal ions. Final purified apoferritin provided no electrochemical signals. pH decrease leads to the opening of apoferritin structure and entering the silver(I) ions. pH increasing causes closure of apoferritin structure without release of metal ions from the structure. Subsequent change in pH enables repeated opening of the apoferritin structure under ions release. Our experiment demonstrated that addition of acetate buffer (pH 5.0) leads to releasing of silver(I) ions and their concentration was then electrochemically detected. Silver(I) ions in given concentrations (0, 7.5, 15, 30 and 60 μM) applied together with apoferritin were enclosed in apoferritin structure in linear dependence. In addition, silver(I) ions released from apoferritin structure were well

determinable. Well detectable signal of silver(I) ions at +0.2 V is shown in DP voltammograms in inset in Fig. 5.

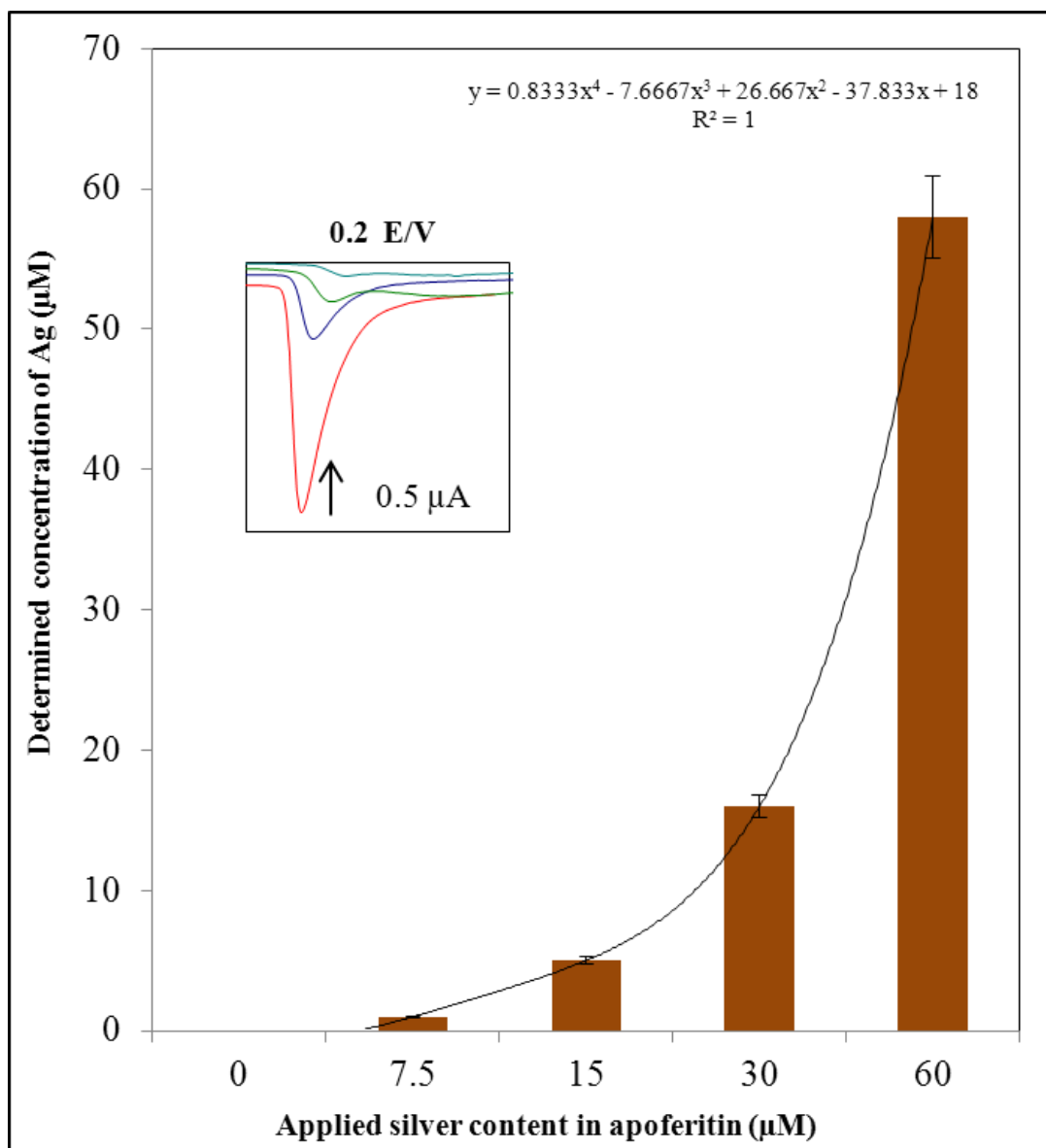


Figure 5. Influence of Ag(I) concentration on determined silver concentration after encapsulation of these ions in apoferritin; in inset: typical DP voltammograms of silver(I) ions after their releasing from apoferritin structure.

Detected amount of silver(I) ions was dramatically reduced at low concentrations of applied silver(I) ions (only 13 %). At highest concentration of applied silver(I) ions, detected concentration of these ions was higher than 95 % (Fig. 5). Obtained dependence confirms the fact that apoferritin

structure may be effectively used for transfer of silver ions. Observed effect is induced by resulting dilution of silver(I) ions and probably also by further interactions of silver(I) ions with apoferritin structure.

3.3 Biotechnological application of silver(I) ions

Tools of targeted therapy including nanotechnological ones are intensively searched [79,80]. Apoferritin structure can be modified in the direction of that kind of the bond onto the surface of the pathogen. In the experiment, we focused on verifying the possibility of using apoferritin molecules to transport silver(I) ions directly to a pathogen. Culture of *S. aureus* was supplemented by apoferritin (0.25 mg/ml) in combination with silver(I) ions in the concentrations of 0, 7.5, 15, 30 and 60 μM . Bacterial culture of *S. aureus* was cultivated in the cultivation medium to the exponential growth phase, when it was subsequently used in the experiment (OD_{600} 0.1). During the first hour of cultivation, there were no significant changes in the growth characteristics. First obvious changes were observable after 1.5 h long cultivation (Fig. 6). Bacterial culture supplemented by the highest concentration of silver(I) ions in the combination with apoferritin proved significant growth depression (for more than 30 % compared to control, $p < 0.05$). The most distinct growth changes were observed after 2.5 hour cultivation, where growth reduction was about 10% under the lowest applied concentration and about 30% under the highest applied concentration of silver(I) ions (Fig. 6A). Apoferritin-silver ions concentrations of 7.5 and 15.0 μM induced significantly lower growth depression of *S. aureus* bacterial culture compared to that without silver(I) ions supplementation ($p < 0.05$). Enhancement of bacterial culture growth may be caused by decomposition of apoferritin and utilization of these products as a source of energy and components for bacterial growth. Higher apoferritin-silver(I) ions concentrations as 30 and 60 μM significantly reduced growth of bacterial culture up until third hour of cultivation (Fig. 6A). We also attempted to subtract control growth and plot the growth changes after 2.5 hour long cultivation, where the sharpest changes were observed (Fig. 6B). The significant changes in the growth were determined under 30 and 60 μM of apoferritin-silver(I) ions treatment. Moreover, concentration of free silver(I) ions was determined by differential pulse voltammetry. At the apoferritin-silver(I) ions concentrations, the measured signal of free silver(I) ions was tenfold lower. It was found that the dependence of free silver(I) ions on the apoferritin-silver(I) ions showed the increasing linear course of the following equation $y = 0.0156x + 0.0645$, $R^2 = 0.9973$. Based on the results obtained it can be concluded that silver(I) ions remain enclosed in the apoferritin structure until decomposition of apoferritin by bacterial enzymatic apparatus occurs. Due to this process, silver(I) ions are released, but only locally, with significant antibacterial effect. Inhibition mechanism of silver(I) ions on microorganisms was investigated in two bacterial species Gram-negative *Escherichia coli* and Gram-positive *Staphylococcus aureus*, which were treated with AgNO_3 [81-83]. Similar morphological changes occurred in both *E.coli* and *S. aureus* cells after Ag^+ treatment. The cytoplasm membrane detached from the cell wall. A remarkable electron-light region appeared in

the centres of the cells, which contained condensed DNA. There were also many small electron-dense granules either surrounding the cell wall or depositing inside the cells. The existence of elements of silver and sulphur in the electron-dense granules and cytoplasm detected by X-ray microanalysis suggested the antibacterial mechanism of silver.

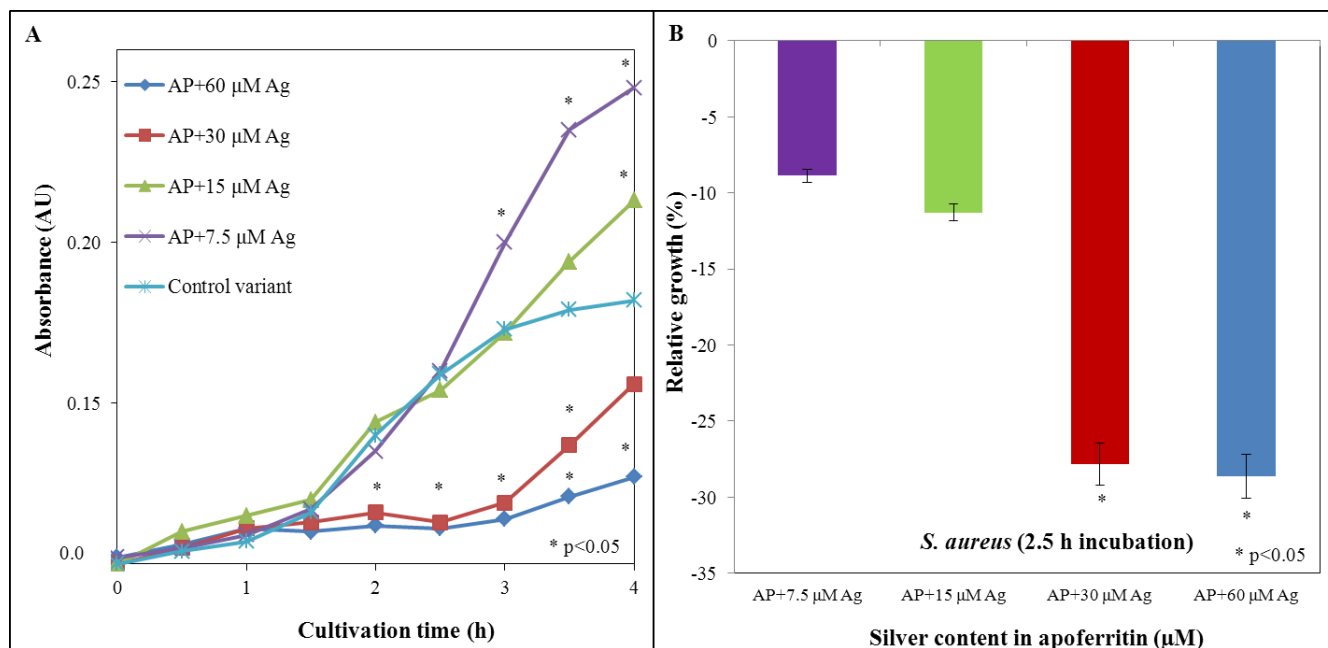


Figure 6. Treatment of *S. aureus* with apoferritin-silver(I) ions complex. (A) Growth curves of *S. aureus* with the addition of apoferritin (AP) and silver(I) ions (Ag) in the active concentration of 7.5, 15, 30 and 60 μM. (B) Changes in the dynamics of *S. aureus* growth after 2.5 hour cultivation in the presence of silver(I) ions with apoferritin. Growth curve of bacterial culture without the silver(I) ions addition has been subtracted.

DNA lost its replication ability and the protein became inactivated after Ag⁺ treatment. The slighter morphological changes of *S. aureus* compared with *E. coli* recommended a defence system of *S. aureus* against the inhibitory effects of Ag⁺ ions [81-83]. The published results in combination with our suggested way how to transport silver(I) ions could be of great interest for new antibacterial strategies.

4. CONCLUSIONS

Biotechnological applications based on nanotechnology approaches are modern tools for the targeted transport of active compounds/drugs with only minimal risk and possible damage to the non-

targeted cells and tissues. These can serve not only for transporting of the drug, but also for targeting of bacteria. In this study, we investigated the possibility to encapsulate silver(I) ions into apoferritin. Suggested apoferritin-based silver(I) ion carrier has potential application in therapeutic targeting to bacterial cells because of significant negative effect on bacterial culture of *S. aureus*.

ACKNOWLEDGEMENTS

Financial support from TACR TA01010088 and CEITEC CZ.1.05/1.1.00/02.0068 is highly acknowledged.

References

1. T. Li, B. Albee, M. Alemayehu, R. Diaz, L. Ingham, S. Kamal, M. Rodriguez and S. W. Bishnoi, *Anal. Bioanal. Chem.*, 398 (2010) 689.
2. A. Bianchini and C. M. Wood, *Environ. Toxicol. Chem.*, 22 (2003) 1361.
3. S. Krizkova, V. Adam and R. Kizek, *Chem. Listy*, 103 (2009) 559.
4. M. Mirzaei and J. Saeed, *Spectroc. Acta Pt. A-Molec. Biomolec. Spectr.*, 82 (2011) 351.
5. J. Kumpiene, E. Brannvall, R. Taraskevicius, C. Aksamitauskas and R. Zinkute, *J. Geochem. Explor.*, 108 (2011) 15.
6. T. Shamspur, M. H. Mashhadizadeh and I. Sheikshoaie, *J. Anal. At. Spectrom.*, 18 (2003) 1407.
7. S. Saeki, M. Kubota and T. Asami, *Int. J. Environ. Anal. Chem.*, 64 (1996) 179.
8. H. S. Kim and M. C. Jung, *Environ. Geochem. Health*, 34 (2012) 55.
9. A. Amine, H. Mohammadi, I. Bourais and G. Palleschi, *Biosens. Bioelectron.*, 21 (2006) 1405.
10. D. Ogoczyk, L. Tymecki, I. Wyzkiewicz, R. Koncki and S. Glab, *Sens. Actuator B-Chem.*, 106 (2005) 450.
11. H. Louie, C. Wong, Y. J. Huang and S. Fredrickson, *Anal. Methods*, 4 (2012) 522.
12. R. M. Abdul, L. Mutnuri, P. J. Dattatreya and D. A. Mohan, *Environ. Monit. Assess.*, 184 (2012) 1581.
13. M. Galiova, J. Kaiser, K. Novotny, J. Novotny, T. Vaculovic, M. Liska, R. Malina, K. Stejskal, V. Adam and R. Kizek, *Appl. Phys. A-Mater. Sci. Process.*, 93 (2008) 917.
14. J. Wang, J. M. Lu and P. A. M. Farias, *Anal. Chim. Acta*, 318 (1996) 151.
15. S. Krizkova, O. Krystofova, L. Trnkova, J. Hubalek, V. Adam, M. Beklova, A. Horna, L. Havel and R. Kizek, *Sensors*, 9 (2009) 6934.
16. S. Krizkova, P. Ryant, O. Krystofova, V. Adam, M. Galiova, M. Beklova, P. Babula, J. Kaiser, K. Novotny, J. Novotny, M. Liska, R. Malina, J. Zehnalek, J. Hubalek, L. Havel and R. Kizek, *Sensors*, 8 (2008) 445.
17. P. Majzlik, A. Strasky, V. Adam, M. Nemecek, L. Trnkova, J. Zehnalek, J. Hubalek, I. Provaznik and R. Kizek, *Int. J. Electrochem. Sci.*, 6 (2011) 2171.
18. L. Trnkova, V. Adam, J. Hubalek, P. Babula and R. Kizek, *Sensors*, 8 (2008) 5619.
19. L. Trnkova, I. Fabrik, D. Huska, H. Skutkova, M. Beklova, J. Hubalek, V. Adam, I. Provaznik and R. Kizek, *J. Environ. Monit.*, 13 (2011) 2763.
20. L. Trnkova, R. Kizek and O. Dracka, *Bioelectrochemistry*, 55 (2002) 131.
21. R. Mikelova, J. Baloun, J. Petrlova, V. Adam, L. Havel, H. Petrek, A. Horna and R. Kizek, *Bioelectrochemistry*, 70 (2007) 508.

22. O. Zitka, D. Huska, V. Adam, A. Horna, M. Beklova, Z. Svobodova and R. Kizek, *Int. J. Electrochem. Sci.*, 5 (2010) 1082.
23. J. Hubalek, J. Prasek, D. Huska, M. Adamek, O. Jasek, V. Adam, L. Trnkova, A. Horna and R. Kizek, in J. Brugger, D. Briand (Editors), Proceedings of the Eurosensors XXIII Conference, 2009, p. 1011.
24. D. Huska, S. Krizkova, J. Hubalek, V. Adam, M. Beklova, L. Trnkova and R. Kizek, *Toxicol. Lett.*, 180 (2008) S236.
25. R. Kizek, L. Trnkova, S. Sevcikova, J. Smarda and F. Jelen, *Anal. Biochem.*, 301 (2002) 8.
26. K. Vytras, I. Svancara and R. Metelka, *J. Serb. Chem. Soc.*, 74 (2009) 1021.
27. I. Svancara, A. Walcarius, K. Kalcher and K. Vytras, *Cent. Eur. J. Chem.*, 7 (2009) 598.
28. L. Trnkova, S. Krizkova, V. Adam, J. Hubalek and R. Kizek, *Biosens. Bioelectron.*, 26 (2011) 2201.
29. J. Petrlova, S. Krizkova, O. Zitka, J. Hubalek, R. Prusa, V. Adam, J. Wang, M. Beklova, B. Sures and R. Kizek, *Sens. Actuator B-Chem.*, 127 (2007) 112.
30. S. Krizkova, D. Huska, M. Beklova, J. Hubalek, V. Adam, L. Trnkova and R. Kizek, *Environ. Toxicol. Chem.*, 29 (2010) 492.
31. K. Stejskal, S. Krizkova, V. Adam, B. Sures, L. Trnkova, J. Zehnalek, J. Hubalek, M. Beklova, P. Hanustiak, Z. Svobodova, A. Horna and R. Kizek, *IEEE Sens. J.*, 8 (2008) 1578.
32. A. Gonzalez-Bellavista, S. Atrian, M. Munoz, M. Capdevila and E. Fabregas, *Talanta*, 77 (2009) 1528.
33. I. Sondi and B. Salopek-Sondi, *J. Colloid Interface Sci.*, 275 (2004) 177.
34. S. Pal, Y. K. Tak and J. M. Song, *Appl. Environ. Microbiol.*, 73 (2007) 1712.
35. S. Efrima and B. V. Bronk, *J. Phys. Chem. B*, 102 (1998) 5947.
36. A. Gauger, M. Mempel, A. Schekatz, T. Schafer, J. Ring and D. Abeck, *Dermatology*, 207 (2003) 15.
37. N. Stobie, B. Duffy, D. E. McCormack, J. Colreavy, M. Hidalgo, P. McHale and S. J. Hinder, *Biomaterials*, 29 (2008) 963.
38. A. Nanda and M. Saravanan, *Nanomed.-Nanotechnol. Biol. Med.*, 5 (2009) 452.
39. W. R. Li, X. B. Xie, Q. S. Shi, S. S. Duan, Y. S. Ouyang and Y. B. Chen, *Biomaterials*, 24 (2011) 135.
40. K. M. Tarquinio, N. K. Kothurkar, D. Y. Goswami, R. C. Sanders, A. L. Zaritsky and A. M. LeVine, *Int. J. Nanomed.*, 5 (2010) 177.
41. A. Khan, M. Qamar and M. Muneer, *Chem. Phys. Lett.*, 519-20 (2012) 54.
42. A. Panacek, L. Kvitek, R. Prucek, M. Kolar, R. Vecerova, N. Pizurova, V. K. Sharma, T. Nevecna and R. Zboril, *J. Phys. Chem. B*, 110 (2006) 16248.
43. G. C. Ford, P. M. Harrison, D. W. Rice, J. M. A. Smith, A. Treffry, J. L. White and J. Yariv, *Philos. Trans. R. Soc. Lond. Ser. B-Biol. Sci.*, 304 (1984) 551.
44. R. M. Xing, X. Y. Wang, C. L. Zhang, Y. M. Zhang, Q. Wang, Z. Yang and Z. J. Guo, *J. Inorg. Biochem.*, 103 (2009) 1039.
45. A. H. Ma-Ham, H. Wu, J. Wang, X. H. Kang, Y. Y. Zhang and Y. H. Lin, *J. Mater. Chem.*, 21 (2011) 8700.
46. M. Okuda, Y. Suzumoto and I. Yamashita, *Cryst. Growth Des.*, 11 (2011) 2540.
47. F. K. Kalman, S. Geninatti-Crich and S. Aime, *Angew. Chem.-Int. Edit.*, 49 (2010) 612.
48. P. Sanchez, E. Valero, N. Galvez, J. M. Dominguez-Vera, M. Marinone, G. Poletti, M. Corti and A. Lascialfari, *Dalton Transactions* (2009) 800.
49. A. Makino, H. Harada, T. Okada, H. Kimura, H. Amano, H. Saji, M. Hiraoka and S. Kimura, *Nanomed.-Nanotechnol. Biol. Med.*, 7 (2011) 638.

50. X. Y. Liu, Z. Q. Ye, W. Wei, Y. G. Du, J. L. Yuan and D. Ma, *Chem. Commun.*, 47 (2011) 8139.
51. G. D. Liu, H. Wu, J. Wang and Y. H. Lin, *Small*, 2 (2006) 1139.
52. G. D. Liu, H. Wu, A. Dohnalkova and Y. H. Lin, *Anal. Chem.*, 79 (2007) 5614.
53. H. Wu, J. Wang, Z. M. Wang, D. R. Fisher and Y. H. Lin, *J. Nanosci. Nanotechnol.*, 8 (2008) 2316.
54. H. Wu, M. H. Engelhard, J. Wang, D. R. Fisher and Y. H. Lin, *J. Mater. Chem.*, 18 (2008) 1779.
55. G. L. Long and J. D. Winefordner, *Anal. Chem.*, 55 (1983) A712.
56. Z. Papp, V. Guzsvany, I. Svancara and K. Vytras, *Int. J. Electrochem. Sci.*, 6 (2011) 5161.
57. M. Stoces, K. Kalcher, I. Svancara and K. Vytras, *Int. J. Electrochem. Sci.*, 6 (2011) 1917.
58. I. Svancara and J. Zima, *Curr. Org. Chem.*, 15 (2011) 3043.
59. V. Diopan, P. Babula, V. Shestivska, V. Adam, M. Zemlicka, M. Dvorska, J. Hubalek, L. Trnkova, L. Havel and R. Kizek, *J. Pharm. Biomed. Anal.*, 48 (2008) 127.
60. R. Kizek, M. Masarik, K. J. Kramer, D. Potesil, M. Bailey, J. A. Howard, B. Klejdus, R. Mikelova, V. Adam, L. Trnkova and F. Jelen, *Anal. Bioanal. Chem.*, 381 (2005) 1167.
61. S. Krizkova, V. Hrdinova, V. Adam, E. P. J. Burgess, K. J. Kramer, M. Masarik and R. Kizek, *Chromatographia*, 67 (2008) S75.
62. J. Petrlova, S. Krizkova, V. Supalkova, M. Masarik, V. Adam, L. Havel, K. J. Kramer and R. Kizek, *Plant Soil Environ.*, 53 (2007) 345.
63. J. Petrlova, M. Masarik, D. Potesil, V. Adam, L. Trnkova and R. Kizek, *Electroanalysis*, 19 (2007) 1177.
64. J. Prasek, J. Hubalek, M. Adamek and R. Kizek, in 2006 IEEE Sensors, Vols 1-3, 2006, p. 1261.
65. V. Shestivska, V. Adam, J. Prasek, T. Macek, M. Mackova, L. Havel, V. Diopan, J. Zehnalek, J. Hubalek and R. Kizek, *Int. J. Electrochem. Sci.*, 6 (2011) 2869.
66. M. C. Radulescu, A. Chira, M. Radulescu, B. Bucur, M. P. Bucur and G. L. Radu, *Sensors*, 10 (2010) 11340.
67. S. Girousi and Z. Stanic, *Curr. Anal. Chem.*, 7 (2011) 80.
68. P. V. Bernhardt, *Aust. J. Chem.*, 59 (2006) 233.
69. K. Jiao, X. Z. Zhang, G. Y. Xu and W. Sun, *Acta Chim. Sin.*, 63 (2005) 1100.
70. G. G. Wildgoose, C. E. Banks, H. C. Leventis and R. G. Compton, *Microchim. Acta*, 152 (2006) 187.
71. X. Z. Ye, Q. H. Yang, Y. Wang and N. Q. Li, *Talanta*, 47 (1998) 1099.
72. J. Tashkhourian, S. Javadi and F. N. Ana, *Microchim. Acta*, 173 (2011) 79.
73. J. Prasek, J. Drbohlavova, J. Chomoucka, J. Hubalek, O. Jasek, V. Adam and R. Kizek, *J. Mater. Chem.*, 21 (2011) 15872.
74. J. Prasek, D. Huska, O. Jasek, L. Zajickova, L. Trnkova, V. Adam, R. Kizek and J. Hubalek, *Nanoscale Res. Lett.*, 6 (2011) 1.
75. S. B. Hocevar and B. Ogorevc, *Talanta*, 74 (2007) 405.
76. X. Z. Zhang, Y. Cui, Z. L. Lv, M. Li, S. S. Ma, Z. G. Cui and Q. Kong, *Int. J. Electrochem. Sci.*, 6 (2011) 6063.
77. A. Celebanska, D. Tomaszewska, A. Lesniewski and M. Opallo, *Biosens. Bioelectron.*, 26 (2011) 4417.
78. S. Shahrokhian and E. Asadian, *Electrochimica Acta*, 55 (2010) 666.
79. J. Chomoucka, J. Drbohlavova, D. Huska, V. Adam, R. Kizek and J. Hubalek, *Pharmacol. Res.*, 62 (2010) 144.
80. J. Chomoucka, J. Drbohlavova, M. Masarik, M. Ryvolova, D. Huska, J. Prasek, A. Horna, L. Trnkova, I. Provaznik, V. Adam, J. Hubalek and R. Kizek, *Int. J. Nanotechnol.*, 9 (2012) 746.

81. Q. L. Feng, J. Wu, G. Q. Chen, F. Z. Cui, T. N. Kim and J. O. Kim, *J. Biomed. Mater. Res.*, 52 (2000) 662.
82. A. R. Shahverdi, A. Fakhimi, H. R. Shahverdi and S. Minaian, *Nanomed.-Nanotechnol. Biol. Med.*, 3 (2007) 168.
83. W. K. Jung, H. C. Koo, K. W. Kim, S. Shin, S. H. Kim and Y. H. Park, *Appl. Environ. Microbiol.*, 74 (2008) 2171